Novel high-flux positively charged composite membrane incorporating titanium-based MOFs for heavy metal removal

Xin-Yu Gong [a], Zhi-Hao Huang [a], Hao Zhang [a], Wei-Liang Liu [a], Xiao-Hua Ma[*,a], Zhen-Liang Xu [a] and Chuyang Y. Tang [b]

[a] *Shanghai Key Laboratory of Multiphase Materials Chemical Engineering, Membrane Science and Engineering R&D Lab, Chemical Engineering Research Center, School of Chemical Engineering, East China University of Science and Technology, 130 Meilong Road, 200237, Shanghai, China*

[b] *Department of Civil Engineering, the University of Hong Kong, Pokfulam Road, Hong Kong S.A.R., China*

Abstract: In this study, a novel positively charged nanofiltration (NF) membrane was fabricated by incorporating metal-organic frameworks (MOFs) into polyethyleneimine (PEI) and trimesic acid (TMA) cross-linking system. NH_2-MIL-125(Ti) provides preferential water channels to improve the permeability of the composite membrane. The effects of NH_2-MIL-125(Ti) loading on the membrane morphology, structure and properties were investigated by ATR-FTIR, SEM, EDS, AFM, Zeta potential measurements, *etc*. Studies have shown that the optimal preparation condition was determined at 0.010 wt% NH_2-MIL-125(Ti) loading. The prepared membrane exhibited a high permeability of 12.2 $L \cdot m^{-2} \cdot h^{-1} \cdot bar^{-1}$ and a $NiCl_2$ rejection of 90.9%. Compared with the pristine composite membrane, the membrane with appropriate amount of NH_2-MIL-125(Ti) greatly improved the permeability (369.2%). The combination of NH_2-MIL-125(Ti) and PEI/TMA cross-linking system has positive significance for the heavy metal wastewater treatment industry.

Keywords: Positive charge, Nanofiltration, Metal-organic frameworks, Cross-linking, Heavy metal

* To whom all correspondence should be addressed.
Email: xiaohuama@ecust.edu.cn.
Tel.: +86 21 64253670; fax: +86 21 64252989.

1. Introduction

Industrial wastewaters often contain toxic heavy metals, which can cause serious threats to ecology and human health [1-4]. Therefore, the removal of heavy metals from industrial wastewater is of vital importance. Nanofiltration (NF) has been proved to be a promising approach to effectively removing heavy metal contaminants from wastewater due to the advantages of high efficiency, low cost and environmental friendliness [5-8].

Conventional NF membranes are a class of thin-film composite (TFC) membranes, composed of a porous support membrane and a selective skin layer with effective pore size of about 1 nm [9, 10]. These NF membranes are typically fabricated through an interfacial polymerization reaction [11, 12]. Although interfacial polymerization has demonstrated many advantages, NF membranes fabricated by this method are usually negatively charged due to the presence of a large amount of unreacted carboxylic acid groups, leading to inefficient separation of heavy metal ions [5]. Thus, exploring positively charged NF membranes is of great interest. Positively charged NF membranes can effectively separate heavy metal cations thanks to the Donnan electrostatic repulsion in addition to the size exclusion effect [6, 13].

Existing studies on the preparation of positively charged NF membranes mainly focus on layer-by-layer assembly [14], grafting [5] and cross-linking [3]. Polyethyleneimine (PEI) is a hydrophilic cationic polyelectrolyte and has been considered as an excellent material for the preparation of highly positively charged membranes [15-17]. Trimesoyl chloride (TMC), gallic acid and trimesic acid (TMA) are often used to cross-link PEI. Compared with other cross-linking agents, TMA has the advantages of low toxicity, easy storage, low price, high water solubility and good stability. However, most NF membranes prepared from PEI have a very dense selection layer,

which limits the permeability. Incorporating suitable amount of Metal-organic frameworks (MOFs) into the composite membrane is an effective way to improve the permeability.

MOFs are a class of porous crystalline materials with three-dimensional (3D) structures composed of metal units and organic ligands. Due to their distinctive characteristics including high surface area, well-defined porosity, and controllable pore structure [18, 19], MOFs have received increasing attention in gas storage [20], drug delivery [21] and catalysis [22]. In addition, MOFs have also been widely used in the field of membrane separation [23-28]. Compared with inorganic nanomaterials, MOFs show superior affinity and compatibility with polymer matrix, preventing formation of non-selective interfacial voids [29]. Furthermore, MOFs embedded in the membrane phase can provide preferential passage for certain molecules, simultaneously selectively excluding unwanted substances according to their features of size, shape, polarity and adaptability [30]. NH_2-MIL-125(Ti) is a porous titanium-based MOFs material containing a cationic functional group (amine group) [31], which can be used to prepare high performance positively charged NF membranes due to its non-toxicity and high hydrophilicity [30, 32, 33]. Currently, there are few studies on NH_2-MIL-125(Ti) in the field of membrane separation, and most of them focus on gas separation. The window size of NH_2-MIL-125(Ti) is approximately 0.6 nm [34], which is larger than the diameter of the water molecule (0.4 nm) and smaller than the hydrated diameter of almost all the heavy metal ions including Ni^{2+} (0.81 nm), Mn^{2+}(0.88 nm) and Zn^{2+}(0.86 nm) [2, 6, 35]. In this regard, NH_2-MIL-125(Ti), as the nanofiller incorporated in the polymeric matrix show great promise in the treatment of wastewater.

Herein, a new and facile technique was used to prepare the PEI/TMA cross-linking membrane, and the NH_2-MIL-125(Ti) was incorporated into the PEI/TMA system to obtain

NH_2-MIL-125(Ti)/PEI/TMA composite membrane. The amount of MOFs added to the composite membrane was optimized systematically. The optimized membrane has excellent separation performance on Ni^{2+} and Mn^{2+}. To our knowledge, this is the first time that NH_2-MIL-125 (Ti) has been combined with a PEI/TMA cross-linking system. This study provides a new idea for the research of heavy metal separation membrane.

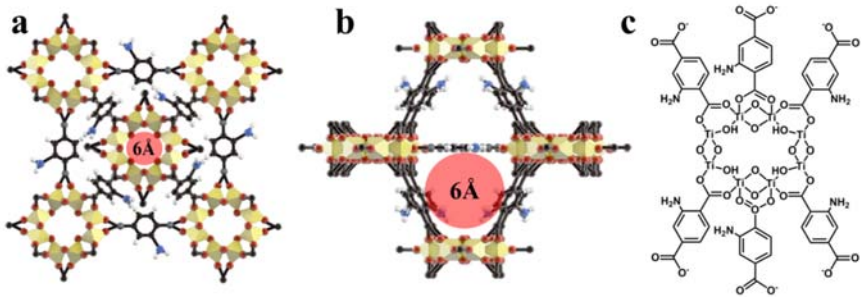

Fig. 1. (a, b) Schematic of NH_2-MIL-125(Ti) structure (H, white; C, black; O, red; N, blue; Ti, yellow polyhedral) and (c) the structural formula of NH_2-MIL-125(Ti).

2. Experiments

2.1. Materials

Tetraethyl titanate ($Ti(OC_2H_5)_4$, 98%), 2-aminoterephthalic acid (NH_2-BDC, 98%), methanol (CH_3OH, ≥99.7%), Ethanol (C_2H_5OH, 99.8%), N, N-dimethylformamide (DMF, 99.8%), inorganic salts ($NiCl_2$, $MnCl_2$, $ZnCl_2$) and poly(ethylene glycol) (PEG) with molecular weight of 400, 800, 1000, and 2000 were provided by Sinopharm Chemical Reagent Co., Ltd. Polyethyleneimine (PEI, Mw ~ 70000, 50% aqueous) and Hexadecyl trimethyl ammonium bromide (CTAB, 99%) were purchased from Shanghai Macklin Biochemical Co., Ltd. Trimesic acid (TMA, ≥99%) were obtained from Adamas-Beta. All chemicals were used without further purification. Deionized water was used throughout the work. Polysulfone (PSF) support membranes with an average molecular weight cut-off (MWCO) of about 50000 Da and a pure water permeability in the range of 200-350

$L^{-1} \cdot m^{-2} \cdot h^{-1} \cdot bar^{-1}$ was provided by Hangzhou Water Treatment Center.

2.2. Synthesis of NH_2-MIL-125(Ti)

The synthesis of NH_2-MIL-125(Ti) was conducted according to the previous reports [36, 37]. Specifically, tetraethyl titanate (1.5 mmol) and NH_2-BDC (6 mmol) were added to a mixed solution of DMF (18 ml) and CH_3OH (2 mL). After stirring at room temperature for 0.5 h, the mixture was poured into a 100 ml Teflon-lined stainless-steel autoclave and heated at 150 °C for 72 h. The resulting yellow suspension was cooled and then centrifuged to obtain the solids. Finally, the solids were washed three times with DMF and CH_3OH, respectively, and dried in an oven at 80 °C overnight.

2.3. Preparation of MOFs/PEI/TMA composite membrane

A certain amount of PEI was dissolved in deionized water to obtain a PEI solution with a concentration of 0.6 wt%. Then, NH_2-MIL-125(Ti) with different doses (0 - 0.02 wt%) were added to the PEI solution while stirring, followed by ultrasonic treatment for 0.5 h. The TMA solution was prepared by mixing TMA (0.1 wt%) with CTAB (0.15 wt%) in the mixture of ethanol and water (1:1 v/v). Afterwards, a positively charged NF membrane was fabricated through cross-linking methods on the PSF support membrane following the procedures shown in Fig. 2. Firstly, the PSF membrane was fixed in a custom-made PTFE circular frame with an inner and outer diameters of 18 cm and 24 cm, respectively. The NH_2-MIL-125(Ti)/PEI suspension was then poured onto the top surface of the membrane, allowing the liquid to completely cover the effective surface of the membrane. After holding in air for 2 min, the membrane was placed in an oven at 80 °C for 3.5 h. Thereafter, the TMA solution was poured onto the upper surface of the membrane, kept in the air for 5 min, and placed in an oven at 120 °C for 0.5 h. Finally, the

NH_2-MIL-125(Ti)/PEI/TMA composite membrane was obtained and stored in deionized water until use. Name the prepared membrane MPT-x (x represents the loading of MOFs).

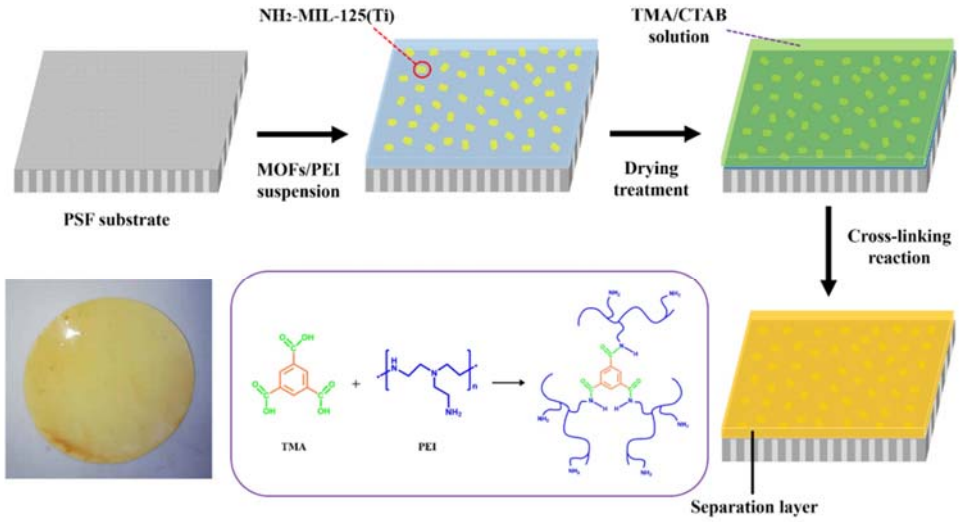

Fig. 2. Schematic of the preparation of NH_2-MIL-125(Ti)/PEI/TMA composite membranes.

2.4. Characterization

The crystalline structure of the synthesized MOFs was characterized by X-ray diffraction (XRD, Bruker, D8 Advance) with a copper target and a Links energy dispersive array detector. Fourier transform infrared spectrometer (FT-IR, Thermo Nicolet, Nicolet-6700) was used to characterize the chemical composition of the synthesized MOFs and the fabricated membranes. The morphology of NH_2-MIL-125(Ti) and the surface morphology of the composite membranes were detected by field emission scanning electron microscopy (FE-SEM, FEI, Nova Nano SEM 450). The surface roughness of the membranes was measured by atomic force microscopy (AFM, Veeco, Nanoscope IIIa Multimode AFM) with a scanning area of 5 μm × 5 μm. QUANTAX 400-30 energy dispersive spectrometer (EDS) installed on the above-mentioned SEM was used to investigate the distribution of MOFs in the composite membranes. The surface charge of the membranes was tested

using zeta potential analyzer (Anton Paar, SurPASS). The hydrophilicity of the membranes was characterized by measuring the static contact angle using a contact angle meter (JC2000A, Shanghai Zhong Cheng Digital Equipment Co., Ltd).

2.5. Membrane performance evaluation

A cross-flow device with an effective filtration area of 27 cm^2 was used to test the separation performance of the NH_2-MIL-125(Ti)/PEI/TMA composite membranes at room temperature. The test pressure was set to 4 bar. Their rejection properties were evaluated by filtration of the heavy metal ions using feed solutions containing 1000 $mg \cdot L^{-1}$ $NiCl_2$, $MnCl_2$ or $ZnCl_2$ without pH adjustment. Prior to the separation test, membranes were pre-pressurized with deionized water for 1 h. The permeability of the composite membrane is calculated by the following formula:

$$Permeability = V / (A \times t \times \Delta p) \quad (1)$$

Where V (L) is the volume of the permeate, A (m^2) is the effective membrane area for the separation test, t (h) is the test time, and Δp (bar) is the test pressure. The calculation of the rejection is defined as:

$$R = (1 - C_p / C_f) \times 100\% \quad (2)$$

where C_f and C_p refer to the solute concentrations in the feed and the permeate, respectively. MWCO of the membrane was analyzed by testing the ability of the composite membranes to reject organic solutes including PEG-400, PEG-800, PEG-1000 and PEG-2000 (200 $mg \cdot L^{-1}$). The salt concentration and the organic solute concentration were measured by an inductively coupled plasma emission spectrometry (ICP) and a total organic carbon analyzer (TOC-L CPH, Shimadzu, Japan), respectively.

3. Results and discussion

3.1. Characterization of NH_2-MIL-125(Ti)

To confirm the successful preparation of NH_2-MIL-125(Ti), we performed a series of characterizations including XRD, FT-IR and SEM. The XRD spectrum (Fig. 3(a)) had characteristic peaks at 2θ of 6.5°, 9.8° and 11.5°, corresponding to the (101), (200) and (211) Miller planes of NH_2-MIL-125(Ti), respectively [33]. Furthermore, the intense FT-IR peak near 3400 cm^{-1} (Fig. 3(b)) can be ascribed to the stretching vibration of the -NH_2 group, consistent with the abundance of -NH_2 groups in NH_2-MIL-125(Ti). The carboxylate coordinated to the Ti-oxo clusters stretch and vibrate in the region of 1400-1650 cm^{-1} [34]. the characteristic peaks in the 1200-1400 cm^{-1} region demonstrated the C-N and C-O structures, and the peaks appearing at 400-700 cm^{-1} indicated the Ti-O vibration [34]. The SEM image (Fig. 3(c)) shows that the most of NH_2-MIL-125(Ti) particles have a disk-like morphology while some of the particles exhibit an irregular polyhedral morphology, which is consistent with the literature [19, 38]. In addition, the particle size ranges from 50 to 600 nm.

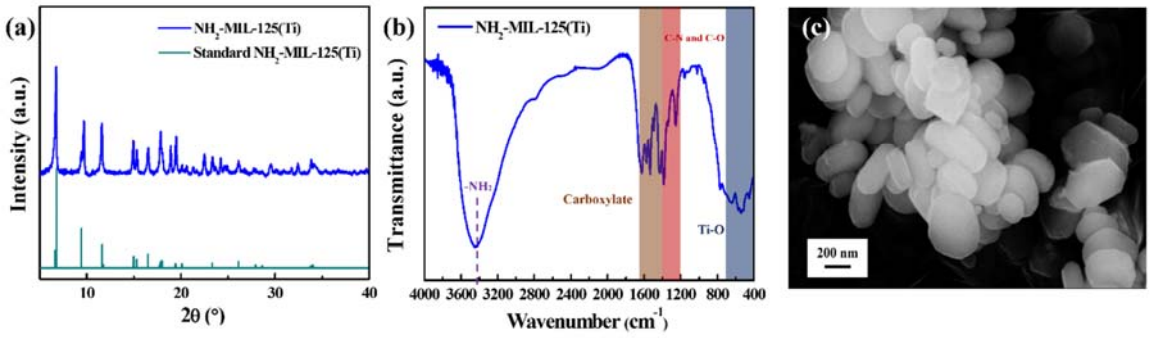

Fig. 3. (a) XRD pattern of NH_2-MIL-125(Ti); (b) FT-IR spectrum of NH_2-MIL-125(Ti); and (c) SEM image of NH_2-MIL-125(Ti).

3.2. Characterization of MOFs/PEI/TMA composite membrane

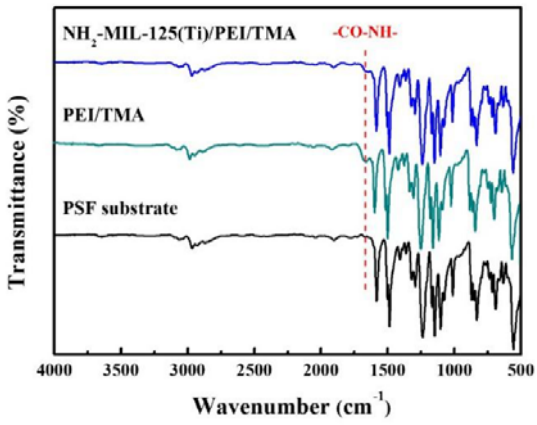

Fig. 4. ATR-FTIR spectra of the PSF substrate, the PEI/TMA membrane and the MPT-0.010 composite membrane.

ATR-FTIR was used to analyze the chemical composition of the PEI/TMA membrane and the MPT-0.010 composite membrane (Fig. 4). The peak at 1668 cm^{-1} is due to the presence of the -CO-NH- groups [39]. This demonstrates the successful cross-linking of $-NH_2$ by TMA.

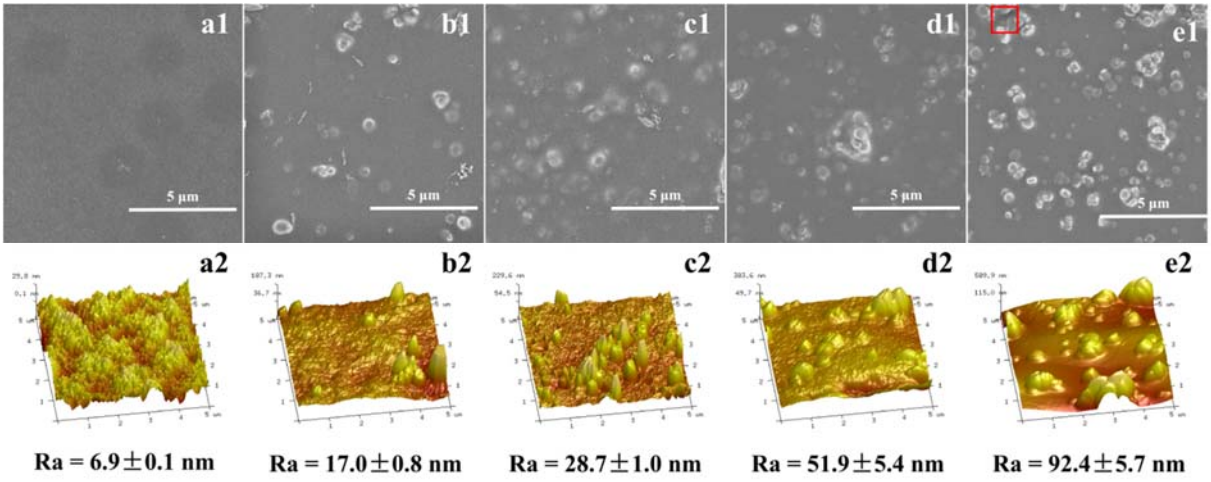

Fig. 5. (1) SEM images and (2) AFM images of the MPT membrane (a: MPT-0; b: MPT-0.005; c: MPT-0.010; d: MPT-0.015; and e: MPT-0.020).

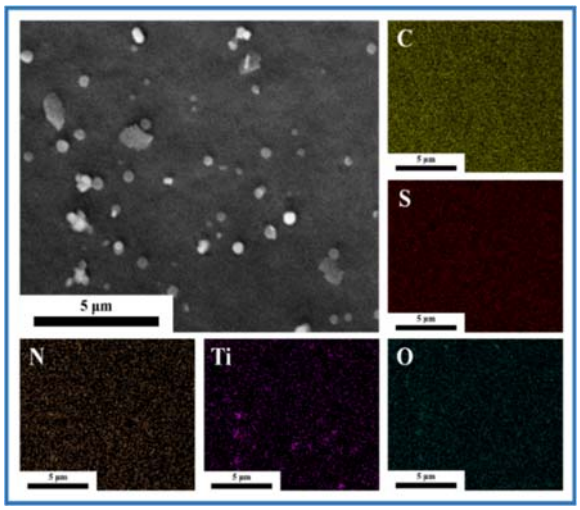

Fig. 6. EDS mapping of the MPT-0.010 composite membrane.

The surface morphologies of MPT composite membranes were observed by FE-SEM (Fig. 5). Greater number of particles were present on the membrane surface at increased MOFs loading (Fig. 5(1)), which were confirmed to be NH_2-MIL-125(Ti) based on EDS characterization (Fig. 6). The NH_2-MIL-125(Ti) particles were relatively uniformly distributed up to a MOFs loading of 0.010 wt% (Fig. 5(a1, b1, c1) and Fig. 6). However, severe particle aggregation became obvious at high MOFs loadings of 0.015 wt% and 0.020 wt% (Fig. 5(d1 and e1)). Defect at the mark was clearly observed. Fig. 5(2) are AFM images of composite membranes prepared with different NH_2-MIL-125(Ti) loadings. Obviously, the roughness of the membrane surface increased as the MOFs loading increases.

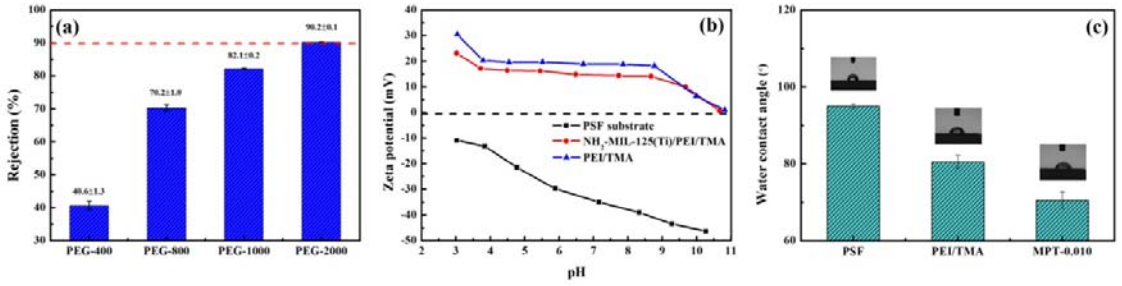

Fig. 7. (a) Selectivity of different PEG solutions (pressure: 4 bar; solute concentration: 200 $mg \cdot L^{-1}$)

by the MPT-0.010 composite membrane; (b) surface potential and (c) static water contact angle of the PSF substrate, the PEI/TMA membrane and the MPT-0.010 composite membrane.

The rejection properties of the MPT-0.010 composite membrane towards PEG molecules with different molecular weight was investigated. As can be seen from Fig. 7(a), the composite membrane had a MWCO in the range of 1000-2000 Da. According to the Stokes radius formula of PEG: $r_s=16.73\times10^{-12}\times M^{0.557}$ (M is the molecular weight of the solute) [40], the effective pore size of the composite membrane was estimated to be in range of 1.5 - 2.2 nm. Therefore, the NH_2-MIL-125(Ti)/PEI/TMA composite membrane prepared with 0.010 wt% MOFs loading can be considered as a loose NF membrane. Furthermore, zeta potential measurements (Fig. 7(b)) show that both the PEI/TMA composite membrane and the NH_2-MIL-125(Ti)/PEI/TMA composite membrane were positively charged over a wide pH range, which can be largely attributed to the protonation of amine groups. The change in water contact angle of cross-linking layer shown in Fig. 7(c) is attributed to the successful incorporation of NH_2-MIL-125(Ti) to improve the hydrophilicity.

3.3. Separation performance of MOFs/PEI/TMA composite membrane

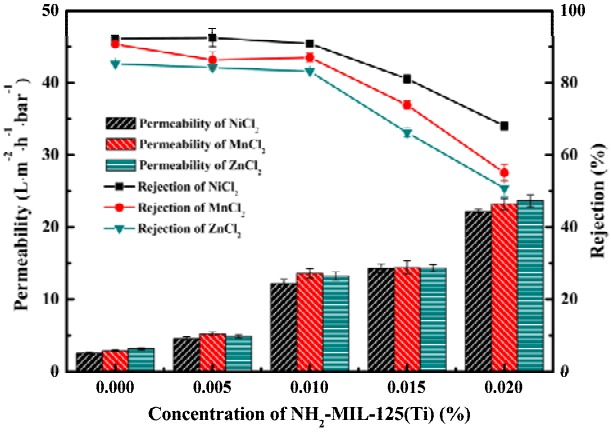

Fig. 8. The effect of NH_2-MIL-125(Ti) loading on heavy metal removal performance of

NH_2-MIL-125(Ti)/PEI/TMA composite membranes.

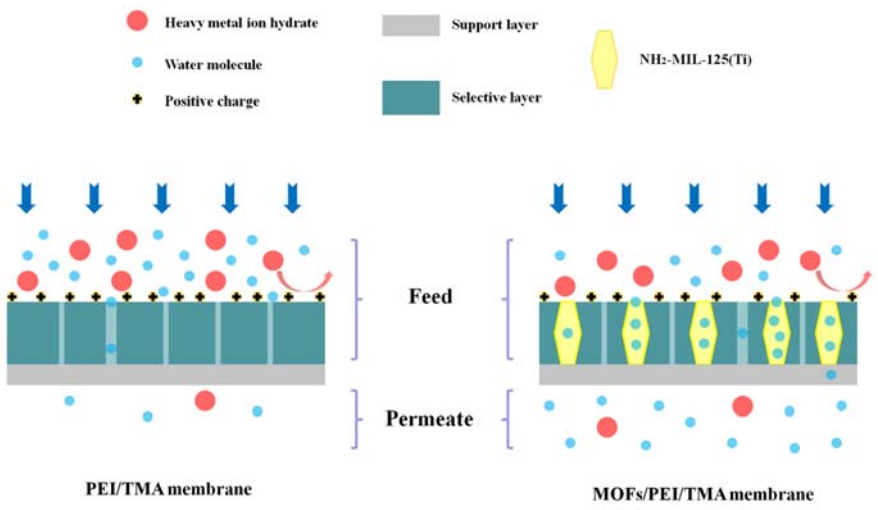

Fig. 9. Schematic diagram of preferential water channels in composite membrane.

Separation performance tests were carried out on NH_2-MIL-125(Ti)/PEI/TMA composite membranes with different NH_2-MIL-125(Ti) loadings (Fig. 8). When the loading amount increased from 0 to 0.010 wt%, membrane permeability increased by approximately 3-4 times (e.g., 2.6 $L \cdot m^{-2} \cdot h^{-1} \cdot bar^{-1}$ at 0 wt% and 12.2 $L \cdot m^{-2} \cdot h^{-1} \cdot bar^{-1}$ at 0.010 wt% using a 1000 $mg \cdot L^{-1}$ feed solution). At the same time, the rejection of heavy metal ions was generally well maintained. This is mainly because NH_2-MIL-125(Ti) provides preferential water channels for the composite membrane (Fig. 9) [41]. As mentioned above, NH_2-MIL-125(Ti) has a suitable window size, which can selectively cut off heavy metal ions and let water molecules pass through. Furthermore, the positive charged nature of NH_2-MIL-125(Ti) helped in retaining rejection [8, 26]. At further increased MOFs loading (0.015 wt% and 0.020 wt%), membrane rejection was severely impaired even though the permeability continued to increase. At these MOFs loadings, the aggregation of the particles became more prominent (Fig. 5(d1 and e1)), which may promote the formation of more defects in the membranes.

In summary, the appropriate NH_2-MIL-125(Ti) loading can improve the separation performance of the PEI/TMA cross-linking membrane. Studies have shown that the MPT-0.010 composite membrane has the best separation performance (permeability: 12.2 $L \cdot m^{-2} \cdot h^{-1} \cdot bar^{-1}$, Ni^{2+} rejection: 90.9%).

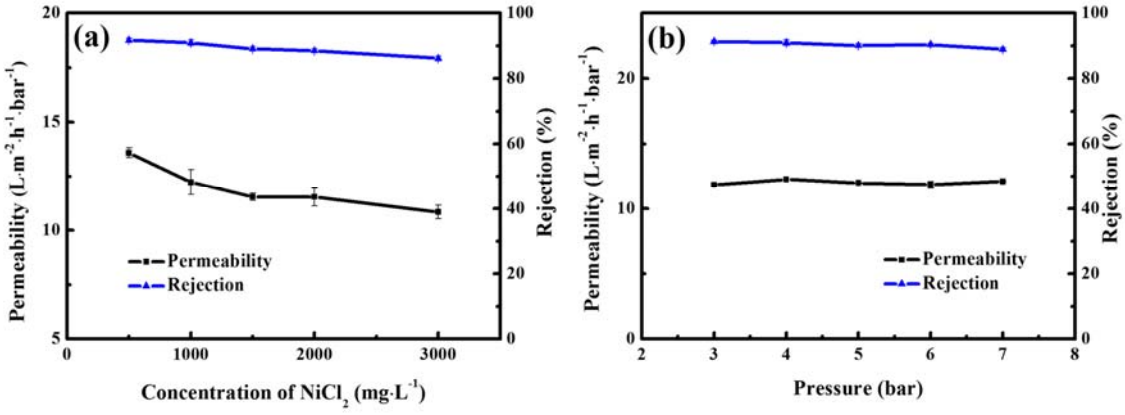

Fig. 10. Heavy metal (Ni^{2+}) removal performance of the MPT-0.010 composite membrane at different (a) feed concentrations (test pressure: 4 bar) and (b) test pressures (salt concentration: 1000 $mg \cdot L^{-1}$).

Fig. 10(a) shows the separation performance of the MPT-0.010 composite membranes at different $NiCl_2$ solution feed concentrations. When the feed concentration was increased from 500 to 3000 $mg \cdot L^{-1}$, the rejection of the composite membrane showed a slight decrease. The permeability of the salt solution decreased as the feed concentration increases, which can be explained by the Spiegler-Kedem model [42]. Meanwhile, higher Cl^- concentration strengthens the electrostatic shielding effect and thereby weakens the Donnan exclusion, resulting in a decrease in rejection [6, 43]. Moreover, the reduction in the size of the hydrated ions at high concentrations can also result in a decrease in the rejection [2]. Nevertheless, our results show that the MPT-0.010 positively charged composite membrane is still applicable to effectively removing heavy metal ions

even with a high concentration. The ability of the MPT-0.010 composite membrane to treat $NiCl_2$ (1000 $mg \cdot L^{-1}$) solution at different test pressures is shown in Fig. 10(b). By increasing the pressure from 3 to 7 bar, the permeability and the selectivity of Ni^{2+} of the composite membrane was nearly unaffected, confirming that the MPT-0.010 composite membrane had good pressure resistance. This is due to the affinity of MOFs to the polymer and the interaction (cross-linking reaction and hydrogen bonds) between $-NH_2$ and TMA. The MPT-0.010 composite membrane exhibited satisfactory heavy metal removal performance compared to other positively charged NF membranes reported in the literature (Table 1).

Table 1 Comparison among NF membranes used to remove heavy metals in the literature and prepared in this work.

Membrane	Ion	Testing condition	Permeability ($L \cdot m^{-2} \cdot h^{-1} \cdot bar^{-1}$)	Rejection (%)	Ref.
MPT-0.010 composite membrane	Ni^{2+}	1000 $mg \cdot L^{-1}$, 4 bar	12.2	90.9	This work
MPT-0.010 composite membrane	Mn^{2+}	1000 $mg \cdot L^{-1}$, 4 bar	13.6	87.1	This work
Chitosan /PES composite membrane	Ni^{2+}	1000 $mg \cdot L^{-1}$, 10 bar	3.45 (pure water)	96.3	[3]
Polythyleneimine-modified membrane	Ni^{2+}	1000 $mg \cdot L^{-1}$, 10 bar	3.30	95.8	[5]
PAN/SPEB blending TFC membrane	Ni^{2+}	1000 $mg \cdot L^{-1}$, 6 bar	7.62 (pure water)	~95.0	[40]
NF270 commercial membrane	Mn^{2+}	1000 $mg \cdot L^{-1}$, 4 bar	13.2 (pure water)	89.0	[44]
PEI/TMC/P84 membranes	Cd^{2+}	1000 $mg \cdot L^{-1}$, 5 bar	1.74 (pure water)	94.0	[45]
PEI/P84 cross-linking membrane	Pb^{2+}	1000 $mg \cdot L^{-1}$, 13 bar	0.98 (pure water)	91.0	[46]
PIL/PSF composite membrane	Ni^{2+}	5 $mmol \cdot L^{-1}$, 6 bar	7.55 (pure water)	~84.0	[47]
$CoFe_2O_4$/CuO/PES blending membrane	Ni^{2+}	100 $mg \cdot L^{-1}$, 5 bar	6.90 (pure water)	92.0	[48]
HPEI-modified GO&EDA membrane	Ni^{2+}	1000 $mg \cdot L^{-1}$, 1 bar	5.01 (pure water)	96.0	[49]

4. Conclusions

In this work, a novel positively-charged NF membranes were prepared by incorporating NH_2-MIL-125(Ti) into the PEI/TMA thermal cross-linking system. It was observed that more particles appeared on the membrane surface as the NH_2-MIL-125(Ti) loading increased. The analysis of MWCO and Zeta potential show that the separation effect of the membrane is mainly due to the Donnan effect of the composite membrane. Separation performance tests show that the threshold of the amount of MOFs added is 0.010 wt%, and exhibits a high permeability of 12.2 $L \cdot m^{-2} \cdot h^{-1} \cdot bar^{-1}$ and a good Ni^{2+} rejection of 90.9%. The incorporated MOFs is positively charged and provides preferential water channels. This work innovatively employed NH_2-MIL-125(Ti) to fabricate highly-permeable NF membranes for heavy metal removal, which would provide some useful guidelines and directions for the future development of MOFs-based separation membranes.

Acknowledgement

The authors gratefully acknowledge financial support from the National Natural Science Foundation of China (21978081) and the Fundamental Research Funds for the Central Universities (JKA012011001 and JKA012011017).

References

[1] J. Gao, S.P. Sun, W.P. Zhu, T.S. Chung, Chelating polymer modified P84 nanofiltration (NF) hollow fiber membranes for high efficient heavy metal removal, Water Res, 63 (2014) 252-261.

[2] M.Y. Zhou, P. Zhang, L.F. Fang, B.K. Zhu, J.L. Wang, J.H. Chen, H.M. Abdallah, A positively charged tight UF membrane and its properties for removing trace metal cations via electrostatic repulsion mechanism, J Hazard Mater, 373 (2019) 168-175.

[3] S. Zhang, M.H. Peh, Z.W. Thong, T.S. Chung, Thin Film Interfacial Cross-Linking Approach To Fabricate a Chitosan Rejecting Layer over Poly(ether sulfone) Support for Heavy Metal Removal,

Ind Eng Chem Res, 54 (2015) 472-479.

[4] F. Zhang, Y. Zhang, G. Zhang, Z. Yang, D.D. Dionysiou, A. Zhu, Exceptional synergistic enhancement of the photocatalytic activity of SnS 2 by coupling with polyaniline and N-doped reduced graphene oxide, Applied Catalysis B: Environmental, 236 (2018).

[5] Y.W. Qi, L.F. Zhu, X. Shen, A. Sotto, C.J. Gao, J.N. Shen, Polythyleneimine-modified original positive charged nanofiltration membrane: Removal of heavy metal ions and dyes, Sep Purif Technol, 222 (2019) 117-124.

[6] M. Peydayesh, T. Mohammadi, O. Bakhtiari, Water desalination via novel positively charged hybrid nanofiltration membranes filled with hyperbranched polyethyleneimine modified MWCNT, Journal Of Industrial And Engineering Chemistry, 69 (2019) 127-140.

[7] Z.W. Thong, Y. Cui, Y.K. Ong, T.S. Chung, Molecular Design of Nanofiltration Membranes for the Recovery of Phosphorus from Sewage Sludge, Acs Sustainable Chemistry & Engineering, 4 (2016) 5570-5577.

[8] M. Qiu, C.J. He, Efficient removal of heavy metal ions by forward osmosis membrane with a polydopamine modified zeolitic imidazolate framework incorporated selective layer, J Hazard Mater, 367 (2019) 339-347.

[9] L. Yu, J.M. Deng, H.X. Wang, J.D. Liu, Y.T. Zhang, Improved Salts Transportation of a Positively Charged Loose Nanofiltration Membrane by Introduction of Poly(ionic liquid) Functionalized Hydrotalcite Nanosheets, Acs Sustain Chem Eng, 4 (2016) 3292-3304.

[10] L. Yu, Y.T. Zhang, Y.M. Wang, H.Q. Zhang, J.D. Liu, High flux, positively charged loose nanofiltration membrane by blending with poly (ionic liquid) brushes grafted silica spheres, J Hazard Mater, 287 (2015) 373-383.

[11] J.Y. Zhu, M.M. Tian, J.W. Hou, J. Wang, J.Y. Lin, Y.T. Zhang, J.D. Liu, B. Van der Bruggen,

Surface zwitterionic functionalized graphene oxide for a novel loose nanofiltration membrane, J Mater Chem A, 4 (2016) 1980-1990.

[12] M.N. Abu Seman, M. Khayet, N. Hilal, Nanofiltration thin-film composite polyester polyethersulfone-based membranes prepared by interfacial polymerization, J Membrane Sci, 348 (2010) 109-116.

[13] W.Y. Ye, N.J. Bernstein, J.Y. Lin, J. Jordens, S.F. Zhao, C.Y.Y. Tang, B. Van der Bruggen, Theoretical and experimental study of organic fouling of loose nanofiltration membrane, J Taiwan Inst Chem E, 93 (2018) 509-518.

[14] X. Li, C. Liu, W.Q. Yin, T.H. Chong, R. Wang, Design and development of layer-by-layer based low-pressure antifouling nanofiltration membrane used for water reclamation, J Membrane Sci, 584 (2019) 309-323.

[15] W.Z. Qiu, H.C. Yang, L.S. Wan, Z.K. Xu, Co-deposition of catechol/polyethyleneimine on porous membranes for efficient decolorization of dye water, J Mater Chem A, 3 (2015) 14438-14444.

[16] F.Y. Zhao, Y.L. Ji, X.D. Weng, Y.F. Mi, C.C. Ye, Q.F. An, C.J. Gao, High-Flux Positively Charged Nanocomposite Nanofiltration Membranes Filled with Poly(dopamine) Modified Multiwall Carbon Nanotubes, Acs Appl Mater Inter, 8 (2016) 6693-6700.

[17] K.F. Gu, S.H. Wang, Y.H. Li, X.T. Zhao, Y. Zhou, C.J. Gao, A facile preparation of positively charged composite nanofiltration membrane with high selectivity and permeability, Journal Of Membrane Science, 581 (2019) 214-223.

[18] V. Guillerm, D. Kim, J.F. Eubank, R. Luebke, X. Liu, K. Adil, M.S. Lah, M. Eddaoudi, A supermolecular building approach for the design and construction of metal-organic frameworks, Chem Soc Rev, 43 (2014) 6141-6172.

[19] H. Wang, X.Z. Yuan, Y. Wu, G.M. Zeng, X.H. Chen, L.J. Leng, Z.B. Wu, L.B. Jiang, H. Li, Facile synthesis of amino-functionalized titanium metal-organic frameworks and their superior visible-light photocatalytic activity for Cr(VI) reduction, J Hazard Mater, 286 (2015) 187-194.

[20] J.A. Mason, M. Veenstra, J.R. Long, Evaluating metal-organic frameworks for natural gas storage, Chem Sci, 5 (2014) 32-51.

[21] T. Kundu, S. Mitra, P. Patra, A. Goswami, D.D. Diaz, R. Banerjee, Mechanical Downsizing of a Gadolinium(III)-based Metal-Organic Framework for Anticancer Drug Delivery, Chem-Eur J, 20 (2014) 10514-10518.

[22] H. Wang, X.Z. Yuan, Y. Wu, G.M. Zeng, X.H. Chen, L.J. Leng, H. Li, Synthesis and applications of novel graphitic carbon nitride/metal-organic frameworks mesoporous photocatalyst for dyes removal, Appl Catal B-Environ, 174 (2015) 445-454.

[23] S.L. Qiu, M. Xue, G.S. Zhu, Metal-organic framework membranes: from synthesis to separation application, Chem Soc Rev, 43 (2014) 6116-6140.

[24] W.B. Li, Y.F. Zhang, Q.B.A. Li, G.L. Zhang, Metal-organic framework composite membranes: Synthesis and separation applications, Chemical Engineering Science, 135 (2015) 232-257.

[25] X.L. Liu, Y.S. Li, G.Q. Zhu, Y.J. Ban, L.Y. Xu, W.S. Yang, An Organophilic Pervaporation Membrane Derived from Metal-Organic Framework Nanoparticles for Efficient Recovery of Bio-Alcohols, Angewandte Chemie-International Edition, 50 (2011) 10636-10639.

[26] N. Yin, K. Wang, L.Z. Wang, Z.Q. Li, Amino-functionalized MOFs combining ceramic membrane ultrafiltration for Pb (II) removal, Chem Eng J, 306 (2016) 619-628.

[27] J.E. Efome, D. Rana, T. Matsuura, C.Q. Lan, Insight Studies on Metal-Organic Framework Nanofibrous Membrane Adsorption and Activation for Heavy Metal Ions Removal from Aqueous Solution, Acs Applied Materials & Interfaces, 10 (2018) 18619-18629.

[28] J.E. Efome, D. Rana, T. Matsuura, C.Q. Lan, Metal-organic frameworks supported on nanofibers to remove heavy metals, Journal Of Materials Chemistry A, 6 (2018) 4550-4555.

[29] S. Sorribas, P. Gorgojo, C. Tellez, J. Coronas, A.G. Livingston, High Flux Thin Film Nanocomposite Membranes Based on Metal-Organic Frameworks for Organic Solvent Nanofiltration, J Am Chem Soc, 135 (2013) 15201-15208.

[30] X.H. Ma, Z. Yang, Z.K. Yao, Z.L. Xu, C.Y.Y. Tang, A facile preparation of novel positively charged MOF/chitosan nanofiltration membranes, J Membrane Sci, 525 (2017) 269-276.

[31] C.H. Hendon, D. Tiana, M. Fontecave, C. Sanchez, L. D'arras, C. Sassoye, L. Rozes, C. Mellot-Draznieks, A. Walsh, Engineering the Optical Response of the Titanium-MIL-125 Metal-Organic Framework through Ligand Functionalization, J Am Chem Soc, 135 (2013) 10942-10945.

[32] P.G. Ingole, M. Sohail, A.M. Abou-Elanwar, M.I. Baig, J.D. Jeon, W.K. Choi, H. Kim, H.K. Lee, Water vapor separation from flue gas using MOF incorporated thin film nanocomposite hollow fiber membranes, Chem Eng J, 334 (2018) 2450-2458.

[33] H. Liu, J. Zhang, D. Ao, Construction of heterostructured ZnIn2S4@NH2-MIL-125(Ti) nanocomposites for visible-light-driven H-2 production, Appl Catal B-Environ, 221 (2018) 433-442.

[34] S. Daliran, A. Santiago-Portillo, S. Navalon, A.R. Oveisi, M. Alvaro, R. Ghorbani-Vaghei, D. Azarifar, H. Garcia, Cu(II)-Schiff base covalently anchored to MIL-125(Ti)-NH2 as heterogeneous catalyst for oxidation reactions, J Colloid Interf Sci, 532 (2018) 700-710.

[35] M. Chen, K. Shafer-Peltier, S.J. Randtke, E. Peltier, Competitive association of cations with poly(sodium 4-styrenesulfonate) (PSS) and heavy metal removal from water by PSS-assisted ultrafiltration, Chem Eng J, 344 (2018) 155-164.

[36] B.X. Zhang, J.L. Zhang, X.N. Tan, D. Shao, J.B. Shi, L.R. Zheng, J. Zhang, G.Y. Yang, B.X. Han, MIL-125-NH2@TiO2 Core-Shell Particles Produced by a Post-Solvothermal Route for High-Performance Photocatalytic H-2 Production, Acs Appl Mater Inter, 10 (2018) 16418-16423.

[37] B.L. Yan, L.J. Zhang, Z.Y. Tang, M. Al-Mamun, H.J. Zhao, X.T. Su, Palladium-decorated hierarchical titania constructed from the metal-organic frameworks NH2-MIL-125(Ti) as a robust photocatalyst for hydrogen evolution, Appl Catal B-Environ, 218 (2017) 743-750.

[38] X.Y. Guo, H.L. Huang, Y.J. Ban, Q.Y. Yang, Y.L. Xiao, Y.S. Li, W.S. Yang, C.L. Zhong, Mixed matrix membranes incorporated with amine-functionalized titanium-based metal-organic framework for CO2/CH4 separation, J Membrane Sci, 478 (2015) 130-139.

[39] C.Y.Y. Tang, Y.N. Kwon, J.O. Leckie, Effect of membrane chemistry and coating layer on physiochemical properties of thin film composite polyamide RO and NF membranes I. FTIR and XPS characterization of polyamide and coating layer chemistry, Desalination, 242 (2009) 149-167.

[40] T.Z. Jia, J.P. Lu, X.Y. Cheng, Q.C. Xia, X.L. Cao, Y. Wang, W.H. Xing, S.P. Sun, Surface enriched sulfonated polyarylene ether benzonitrile (SPEB) that enhances heavy metal removal from polyacrylonitrile (PAN) thin-film composite nanofiltration membranes, J Membrane Sci, 580 (2019) 214-223.

[41] Y.Y. Zhao, Y.L. Liu, X.M. Wang, X. Huang, Y.F.F. Xie, Impacts of Metal-Organic Frameworks on Structure and Performance of Polyamide Thin-Film Nanocomposite Membranes, Acs Appl Mater Inter, 11 (2019) 13724-13734.

[42] H. Zhang, D. Taymazov, M.P. Li, Z.H. Huang, W.L. Liu, X. Zhang, X.H. Ma, Z.L. Xu, Construction of MoS2 composite membranes on ceramic hollow fibers for efficient water desalination, J Membrane Sci, 592 (2019).

[43] R. Jiraratananon, A. Sungpet, P. Luangsowan, Performance evaluation of nanofiltration

membranes for treatment of effluents containing reactive dye and salt, Desalination, 130 (2000) 177-183.

[44] B.A.M. Al-Rashdi, D.J. Johnson, N. Hilal, Removal of heavy metal ions by nanofiltration, Desalination, 315 (2013) 2-17.

[45] J. Gao, S.P. Sun, W.P. Zhu, T.S. Chung, Green modification of outer selective P84 nanofiltration (NF) hollow fiber membranes for cadmium removal, J Membrane Sci, 499 (2016) 361-369.

[46] J. Gao, S.P. Sun, W.P. Zhu, T.S. Chung, Polyethyleneimine (PEI) cross-linked P84 nanofiltration (NF) hollow fiber membranes for Pb2+ removal, J Membrane Sci, 452 (2014) 300-310.

[47] Y. Tang, B.B. Tang, P.Y. Wu, Preparation of a positively charged nanofiltration membrane based on hydrophilic-hydrophobic transformation of a poly(ionic liquid), J Mater Chem A, 3 (2015) 12367-12376.

[48] F. Zareei, S.M. Hosseini, A new type of polyethersulfone based composite nanofiltration membrane decorated by cobalt ferrite-copper oxide nanoparticles with enhanced performance and antifouling property, Sep Purif Technol, 226 (2019) 48-58.

[49] Y. Zhang, S. Zhang, T.S. Chung, Nanometric Graphene Oxide Framework Membranes with Enhanced Heavy Metal Removal via Nanofiltration, Environ Sci Technol, 49 (2015) 10235-10242.

Figure captions

Fig. 1. (a, b) Schematic of NH_2-MIL-125(Ti) structure (H, white; C, black; O, red; N, blue; Ti, yellow polyhedral) and (c) the structural formula of NH_2-MIL-125(Ti).

Fig. 2. Schematic of the preparation of NH_2-MIL-125(Ti)/PEI/TMA composite membranes.

Fig. 3. (a) XRD pattern of NH_2-MIL-125(Ti); (b) FT-IR spectrum of NH_2-MIL-125(Ti); and (c) SEM image of NH_2-MIL-125(Ti).

Fig. 4. ATR-FTIR spectra of the PSF substrate, the PEI/TMA membrane and the MPT-0.010 composite membrane.

Fig. 5. (1) SEM images and (2) AFM images of the MPT membrane (a: MPT-0; b: MPT-0.005; c: MPT-0.010; d: MPT-0.015; and e: MPT-0.020).

Fig. 6. EDS mapping of the MPT-0.010 composite membrane.

Fig. 7. (a) Selectivity of different PEG solutions (pressure: 4 bar; solute concentration: 200 $mg \cdot L^{-1}$) by the MPT-0.010 composite membrane; (b) surface potential and (c) static water contact angle of the PSF substrate, the PEI/TMA membrane and the MPT-0.010 composite membrane.

Fig. 8. The effect of NH_2-MIL-125(Ti) loading on heavy metal removal performance of NH_2-MIL-125(Ti)/PEI/TMA composite membranes.

Fig. 9. Schematic diagram of preferential water channels in composite membrane.

Fig. 10. Heavy metal (Ni^{2+}) removal performance of the MPT-0.010 composite membrane at different (a) feed concentrations (test pressure: 4 bar) and (b) test pressures (salt concentration: 1000 $mg \cdot L^{-1}$).

Figures

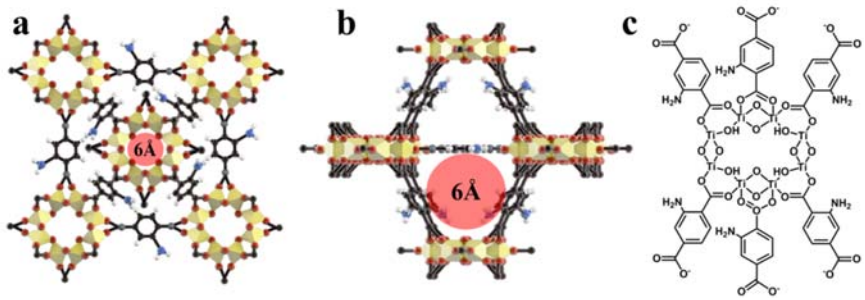

Fig. 1

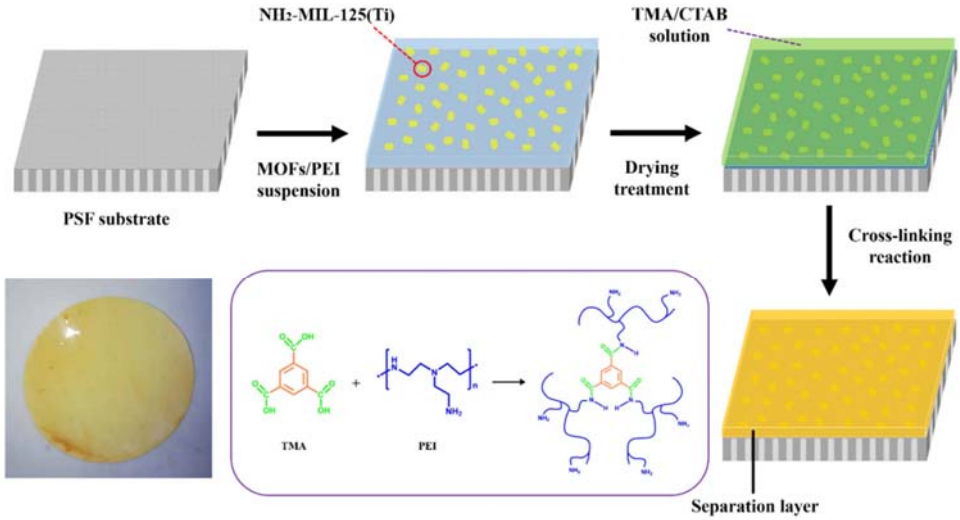
NH2-MIL-125(Ti)
TMA/CTAB solution
MOFs/PEI suspension
Drying treatment
PSF substrate
Cross-linking reaction
TMA
PEI
Separation layer

Fig. 2

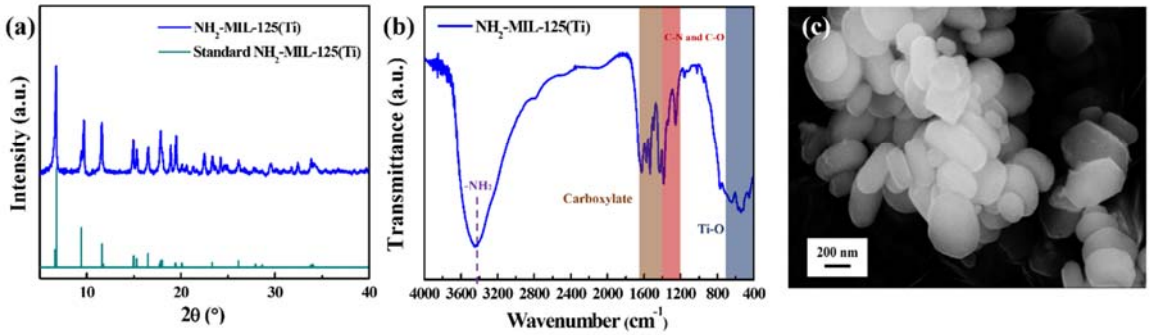
(a)
NH2-MIL-125(Ti)
Standard NH2-MIL-125(Ti)
Intensity (a.u.)
10
20
30
40
2θ (°)
(b)
NH2-MIL-125(Ti)
C-N and C-O
-NH2
Carboxylate
Ti-O
Transmittance (a.u.)
4000 3600 3200 2800 2400 2000 1600 1200 800 400
Wavenumber (cm-1)
(c)
200 nm

Fig. 3

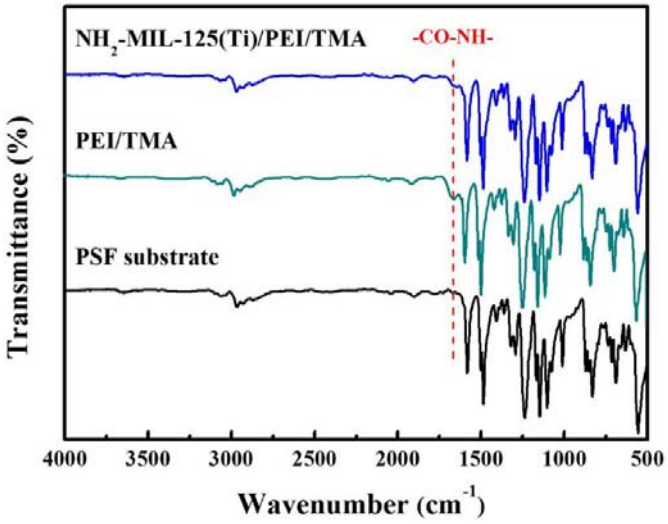
NH2-MIL-125(Ti)/PEI/TMA
-CO-NH-
PEI/TMA
PSF substrate
Transmittance (%)
4000
3500
3000
2500
2000
1500
1000
500
Wavenumber (cm-1)

Fig. 4

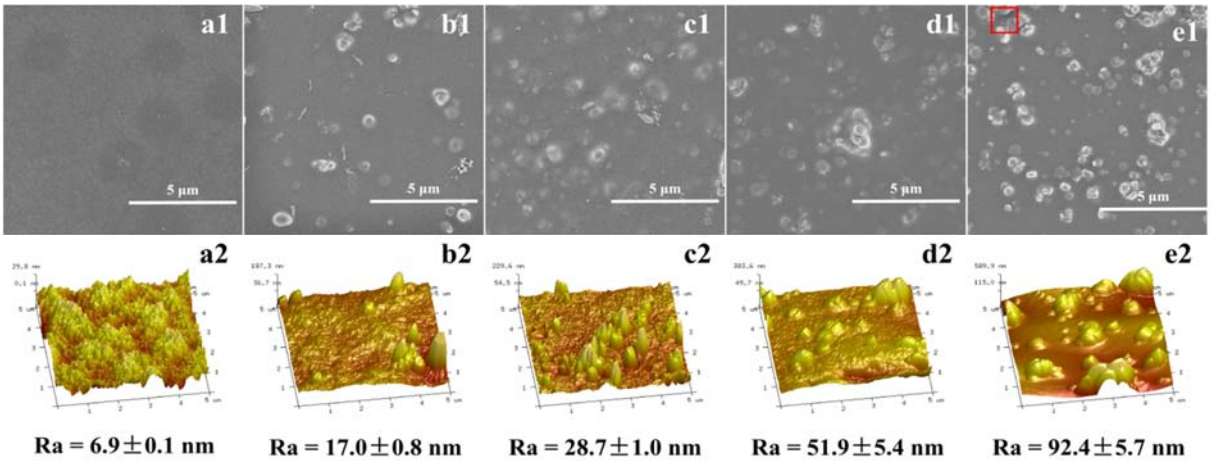
a1
b1
c1
d1
e1
5 μm
a2
b2
c2
d2
e2
Ra = 6.9±0.1 nm
Ra = 17.0±0.8 nm
Ra = 28.7±1.0 nm
Ra = 51.9±5.4 nm
Ra = 92.4±5.7 nm

Fig. 5

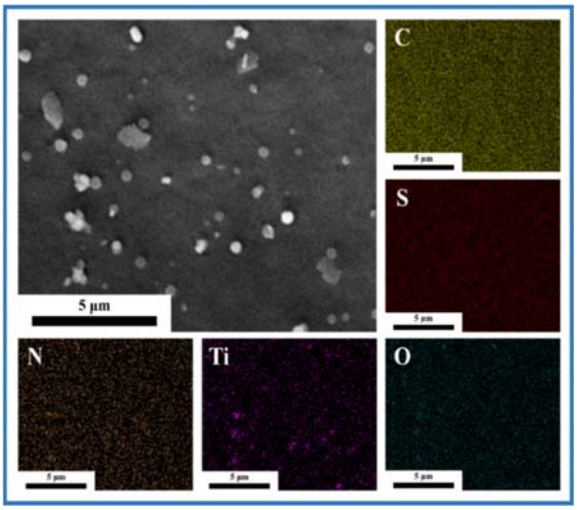

Fig. 6

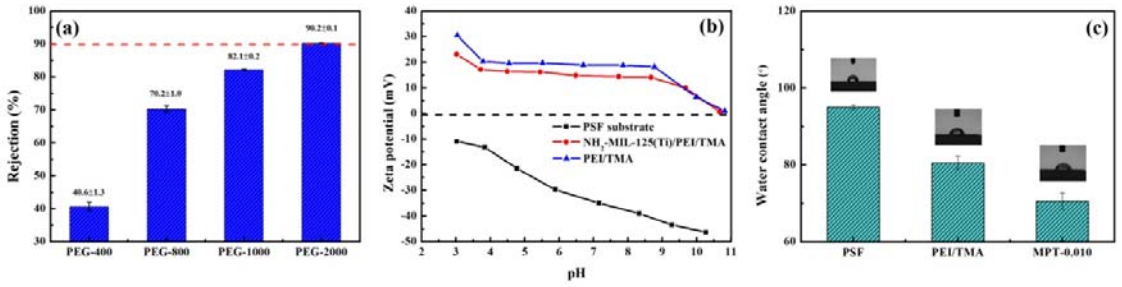
(a)
Rejection (%)
40.6±1.3
70.2±1.0
82.1±0.2
90.2±0.1
PEG-400
PEG-800
PEG-1000
PEG-2000
(b)
Zeta potential (mV)
PSF substrate
NH2-MIL-125(Ti)/PEI/TMA
PEI/TMA
pH
(c)
Water contact angle (°)
PSF
PEI/TMA
MPT-0.010

Fig. 7

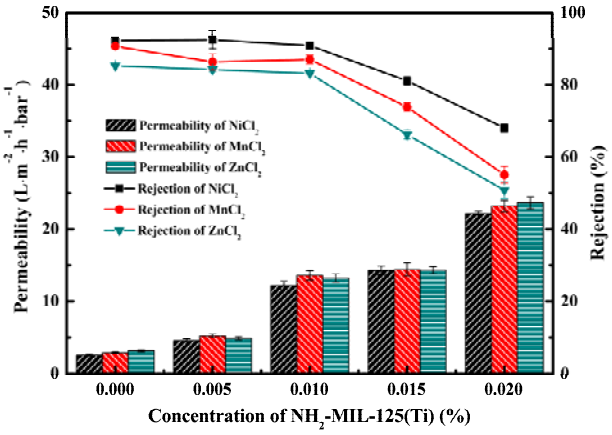
Permeability of NiCl2
Permeability of MnCl2
Permeability of ZnCl2
Rejection of NiCl2
Rejection of MnCl2
Rejection of ZnCl2
Permeability (L·m-2·h-1·bar-1)
Rejection (%)
Concentration of NH2-MIL-125(Ti) (%)
0.000
0.005
0.010
0.015
0.020
0
10
20
30
40
50
0
20
40
60
80
100

Fig. 8

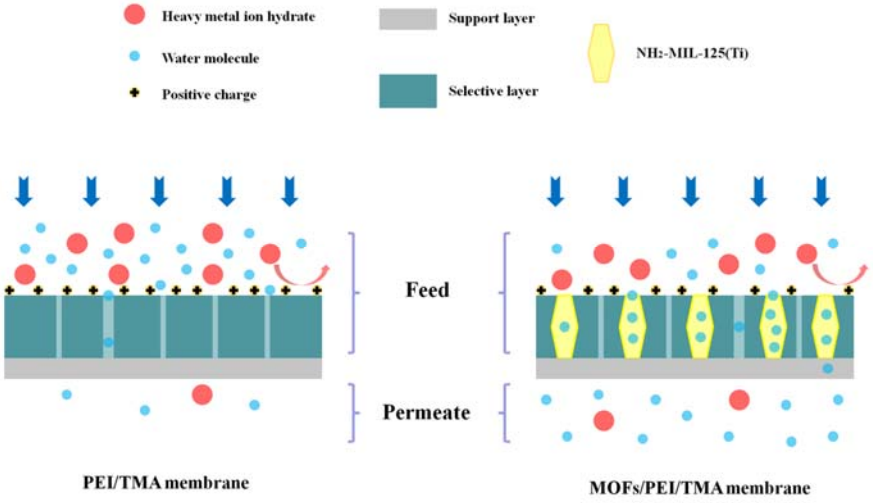
Heavy metal ion hydrate
Water molecule
Positive charge
Support layer
Selective layer
NH2-MIL-125(Ti)
Feed
Permeate
PEI/TMA membrane
MOFs/PEI/TMA membrane

Fig. 9

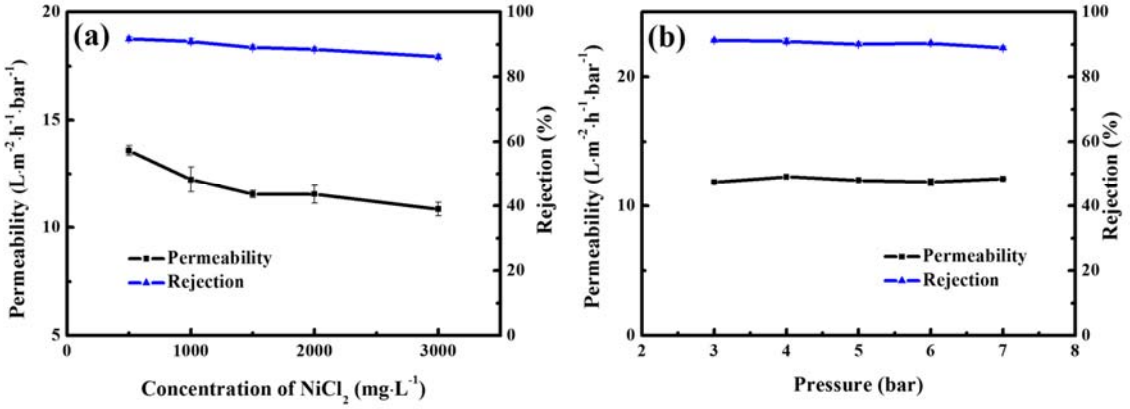
(a)
Permeability (L·m^{-2}·h^{-1}·bar^{-1})
Rejection (%)
Permeability
Rejection
Concentration of NiCl$_2$ (mg·L^{-1})
(b)
Permeability (L·m^{-2}·h^{-1}·bar^{-1})
Rejection (%)
Permeability
Rejection
Pressure (bar)

Fig. 10